

# Dislocation structure of AlN/SiC templates grown by sublimation

© A.E. Kalmykov, A.V. Myasoedov, L.M. Sorokin

Ioffe Institute,  
194021 St. Petersburg, Russia  
E-mail: aekalm@mail.ioffe.ru

Received June 20, 2023

Revised November 6, 2023

Accepted November 6, 2023

The dislocation structure of an AlN layer grown on a SiC substrate by sublimation was studied using transmission electron microscopy. The peculiarity of the growth method was the evaporation of the substrate during the growth of the layer to prevent its cracking. The purpose of the study was to identify the sources of threading dislocations in the AlN layer. Dislocation superjogs, which are sources of dislocations, were found in the layer. A connection between the formation of superjogs and the procedure of substrate evaporation is assumed.

**Keywords:** aluminum nitride, transmission electron microscopy, dislocation, jog.

DOI: 10.61011/SC.2023.08.57617.5333

## 1. Introduction

The heteroepitaxy of thin polar layers of aluminum nitride on substrates (for example, sapphire) is accompanied by the appearance of high densities of threading dislocations (TD) penetrating the layer from the interface to the surface [1]. In the future, homoepitaxy using aluminum nitride substrates should significantly improve the quality of device structures by reducing the TD density, which, in particular, will have a positive effect on the characteristics of widely used UV laser structures based on AlGaIn solid solutions [2]. At the moment, the TD density is high ( $\geq 10^{10} \text{ cm}^{-2}$  [2,3]), which is due to the difference in the lattice constants and thermal expansion coefficient of the substrate (for example, sapphire) and the AlGaIn structure. In the case of using aluminum nitride as a substrate, these differences will obviously be minimized. Currently, the production of aluminum nitride substrates is in its infancy. One promising technology is the growth of bulk AlN crystals using the sublimation method. As part of this method, there are various approaches [4,5]: spontaneous nucleation, heteroepitaxial growth of AlN on foreign substrates (SiC), as well as homoepitaxial growth on seeds obtained by the second method. Differences in the coefficients of thermal expansion and parameters of the crystal lattices of AlN and SiC lead to cracking of the AlN layer during cooling in the growth chamber. A positive result in preventing cracking was achieved by evaporating the substrate during the growth of the AlN [6] layer.

Aluminum nitride crystallizes in the wurtzite structure. This structure is described by a hexagonal crystal lattice. This work examines crystals grown in the polar direction  $\langle 0001 \rangle$ . There are three main types of dislocations in the structure:  $a$ -dislocations with  $\mathbf{b}_a = (a_0/3)\langle 11\bar{2}0 \rangle$ ,  $c$ -dislocations with  $\mathbf{b}_c = c_0\langle 0001 \rangle$  and their combination —  $a + c$  dislocations with  $\mathbf{b}_{a+c} = (1/3)\langle 11\bar{2}3 \rangle$ . Here  $\mathbf{b}$  — Burgers vector,  $a_0$  and  $c_0$  — lattice constants. The defect structures of bulk crystals and thin films of AlN

are noticeably different from each other. The latter are characterized by the appearance of high TD densities that penetrate the film from the interface with the substrate to the surface. In this case, the main contribution to the dislocation density during heteroepitaxy on foreign substrates is made by edge TD with a nonzero  $a$  component, i.e.  $a$ - and  $a + c$ -dislocations.

Transmission electron microscopy (TEM) provides the ability to directly measure TD density without the use of any models. Their almost strict vertical (along the  $\langle 0001 \rangle$  axis) orientation makes it possible to estimate the TD density as the number of TD lines crossing a unit area of the growth surface. In this structure, the method allows one to measure the density of TD  $\geq 10^{10} \text{ cm}^{-2}$ . If dislocations are located in the basal or pyramidal plane, then their density can be estimated as the ratio of their total length to the volume of the sample [7].

A preliminary TEM study [8] showed that the TDs are distributed very unevenly throughout the sample; most of them form equilibrium configurations in the form of dislocation walls. This can be explained by the high mobility of dislocations at the growth temperature 1900–2100°C. Chaotically located dislocations are concentrated in separate, rarely encountered areas with a density of the order of  $1-5 \cdot 10^8 \text{ cm}^{-2}$ . In the sample with an area of  $\sim 5000 \mu\text{m}^2$ , only two such regions were found, each with an area of  $\sim 15 \mu\text{m}^2$ . Apparently, these are TD that are at the stage of forming an equilibrium configuration.

In addition to TDs, dislocations with a  $\langle 0001 \rangle$  slip plane were found in the sample. The purpose of this work is to study dislocation structures formed by dislocations in the basal plane and to clarify their role in the formation of TD.

## 2. Experiment procedure

The growth of AlN crystals was carried out by the sublimation sandwich method in a tantalum carbide crucible

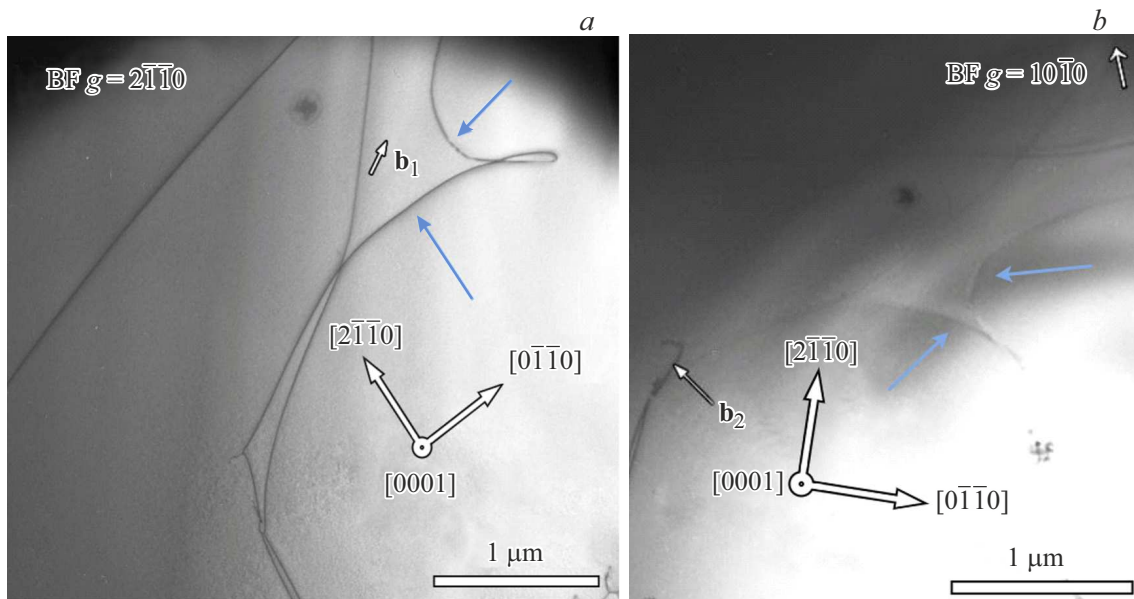


**Figure 1.** TEM image of the superjog region in reflexes  $2\bar{1}\bar{1}0$  (*a*) and  $10\bar{1}0$  (*b*). A dislocation with a superjog corresponds to the Burgers vector  $\mathbf{b}_1$ . (The colored version of the figure is available on-line).

using a silicon carbide substrate as a seed crystal [9]. The substrate was cut from a single-crystal of silicon carbide of the  $6H$  polytype, cylindrical in shape 15 mm in diameter. In order to thin the substrate, it was previously mechanically ground and polished on both sides to a thickness of  $\sim 0.1$ – $1$  mm. To achieve growth,  $C$ -polar orientation ( $000\bar{1}$ ) was used.

The source of AlN was annealed polycrystalline aluminum nitride in the form of a powder placed at the bottom of a tantalum crucible. The SiC seed substrate was located a short distance directly above the source inside the crucible. The rate of growth of aluminum nitride and evaporation of the seed substrate was controlled by adjusting the distance between the source and the substrate. The growth was carried out in an atmosphere of  $N_2$  or Ag under a pressure of  $0.01$ – $1.5$  bar at a temperature of  $1900$ – $2100^\circ\text{C}$ . The duration of the growth process was  $12$ – $20$  h. During the specified time, the thickness of the AlN layer reached a value of  $0.3$ – $1.5$  mm, and the seed substrate was completely removed. The technology of the growth of an AlN crystal is described in more detail in the work [9].

To carry out a TEM study of a bulk single crystal of aluminum nitride, a sample with a thickness of  $\sim 1$  mm was selected. The sample was prepared in planar geometry. The region chosen for the study was near the interface of the crystal and the evaporated SiC substrate. A fragment of size  $2 \times 2$  mm was cut from the selected aluminum nitride crystal, after which it was mechanically thinned to a thickness of  $\sim 30 \mu\text{m}$ . Subsequent thinning was carried out on an ion etching installation using  $\text{Ar}^+$  ions at an accelerating voltage of  $4$  kV until a through hole was formed. Due to the expected low density of defects, in particular the density of dislocations, the main task of

preparing the sample was to obtain a hole of maximum diameter with extensive fields accessible for observation along its perimeter. The TEM study was performed on a Philips EM420 microscope at the Ioffe Institute.

### 3. Experimental results

Figure 1, *a* shows an image of a dislocation consisting of two segments (marked with blue arrows) located in the basal planes ( $0001$ ) of the AlN epitaxial layer. The image was obtained in two-beam conditions with the current diffraction vector  $\mathbf{g} = (2\bar{1}\bar{1}0)$ . In an electron micrograph recorded from the same area of the sample, but with the current diffraction vector  $\mathbf{g} = (10\bar{1}0)$ , the image contrast disappears almost completely (Figure 1, *b*). The residual contrast on dislocations with the Burgers vector  $\mathbf{b}_2$  for reflection  $\mathbf{g} = 0\bar{1}\bar{1}0$  is due to the non-zero contribution of the  $\mathbf{g} \cdot (\mathbf{b} \times \mathbf{l})$  term to the dislocation image contrast, where  $\mathbf{l}$  — the unit tangent vector to the dislocation line. According to the  $(\mathbf{g} \cdot \mathbf{b})$  criterion, the Burgers vector of the dislocation is  $\mathbf{b} = 1/3[1\bar{2}10]$ . The loop formed by the dislocation line (Figure 1, *a*) indicates that here the dislocation is pinned by a compound superjog according to the diagram in Figure 2.

Dislocation segments  $X$  and  $Y$  (indicated by arrows in Figure 1, *a*) are connected by a superjog  $MN$  (Figure 2), i.e. superjog, the value of which significantly exceeds the lattice constant. This value is sufficient for the segments to have little influence on each other through stress fields, not to form a dipole, but to behave independently. As far as we know, a superjog in aluminum nitride has been discovered for the first time. In this case, each of the

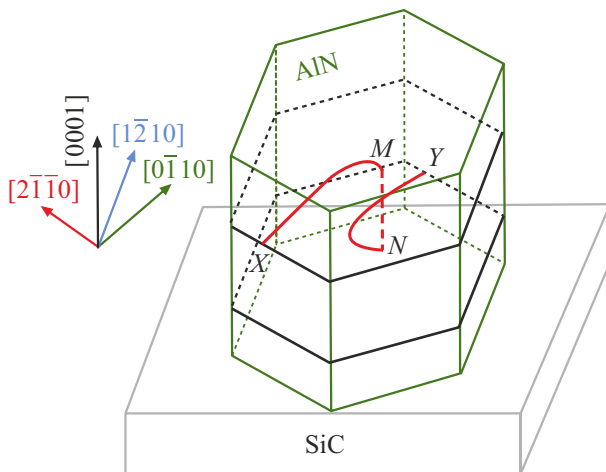


**Figure 2.** Schematic representation of a composite superjog.

segments behaves as a source of dislocations with one fixed point [10], as evidenced by the curved shape of each dislocation segment in Figure 1, *a*. Threshold *MN* is in the prismatic plane, outside the slip plane (0001) and represents a sessile dislocation. Thus, both segments are fixed at points *M* and *N*. The force acting from the external shear stress is always perpendicular to each element of the dislocation line, therefore, both segments, in this case, under the action of the shear stress can only rotate to form a spiral. As the helix unwinds, the total length of the dislocation increases and the dislocation density, defined as the ratio of the total length of dislocations to the volume of the sample, also increases.

Superjogs are formed as a result of double cross-slip under the action of shear stress [10]. The source of the shear stress in the basal plane can apparently be discontinuities in the SiC substrate in the interface region formed during its evaporation. A solid substrate obviously does not create an resolved shear stress in the epitaxial layer, but as soon as sections of the epitaxial layer without a substrate appear at the heterointerface, shear stresses appear in the area of their boundaries. The presence of segment *MN* (Figure 2) clearly indicates the presence of shear stress in the prismatic plane. It is thanks to this stress that the segments *X* and *Y* are spaced far enough from each other to carry out mutually independent sliding in the basal planes, unfolding in spirals. Thus, the superjog is a source of dislocations because it increases the length of dislocation lines in the basal planes.

Let's estimate the value of the superjog *MN*. The radius of curvature *R* of the segment *X* in the equilibrium state is related to the acting shear stress by the relation

$$\tau = \alpha Gb/R, \quad (1)$$

where  $\alpha \approx 0.5-1.0$  [10], Young's modulus is 223 GPa [11], hence the shear modulus  $G = 92.2$  GPa. Accordingly, the magnitude of the shear stress  $\tau$ , which causes the segments to twist into a spiral in the basal plane, lies in the

range  $2.3-4.6 \cdot 10^{-2}$  GPa. An estimate of the maximum stress due to the difference in lattice constants at the heterointerface gives a value of 2.8 GPa, which exceeds  $\tau$  by 2 orders of magnitude. Consequently, the assumption that the increase in the length of dislocations in the basal plane is caused by shear stresses near the boundaries of the residual islands of the substrate is quite plausible. On the other hand, shear stress is associated with the minimum value of the length  $\gamma$  of the segment *MN*, when the segments *X* and *Y* can move independently of each other, by the relation [10]

$$\tau b \geq \frac{0.25Gb^2}{2\pi(1-\nu)\gamma}. \quad (2)$$

Here  $\nu$  — Poisson's ratio,  $\nu = 0.21$  [12]. It follows from relations (1) and (2) that

$$\gamma \geq \frac{0.25R}{2\pi(1-\nu)\alpha}.$$

Therefore, depending on the value of  $\alpha$ , the value of  $\gamma$  lies within the limits of  $0.05-0.1R$ . The value of *R* is  $0.6 \mu\text{m}$  (Figure 1), respectively,  $\gamma \geq 30$  nm. Considering that the thickness of the sample for study by TEM does not exceed 100 nm, it can be argued that the value of the superjog threshold lies in the range from 30 to 100 nm.

Thus, whenever a segment is formed in a dislocation unfolding spiral in the basal plane, parallel to its Burgers vector [10], there appears a non-zero probability of transition (for example, when encountering some obstacle) of this section into prismatic plane to form a half-loop. Vacancies can serve as obstacles, the concentration of which should be high in the forming AlN layer due to the high growth temperature. The half-loop can reach the growth surface by sliding under the action of shear stress, which led to the formation of a superjog (Figure 1).

## 4. Conclusion

Thus, the formation of a superjog in a dislocation propagating in an AlN crystal grown by sublimation on a SiC substrate was discovered for the first time. It is shown that the superjog, under these growth conditions, is a source of dislocations. Superjog segments located in prismatic and pyramidal planes can reach the growth surface, thereby increasing the TD density, which will negatively affect the quality of device structures formed on AlN. Modifying the growth technology by reducing the stage when discontinuities form in the substrate will reduce the dislocation density.

## Acknowledgments

The authors would like to thank E.I. Mokhov for providing the samples. The TEM study was carried out on the equipment of the IPM at the Ioffe Institute.

## Conflict of interest

The authors declare that they have no conflict of interest.

## References

- [1] D.V. Nechaev, O.A. Koshelev, V.V. Ratnikov, P.N. Brunkov, A.V. Myasoedov, A.A. Sitnikova, S.V. Ivanov, V.N. Jmerik. *Superlatt. Microstruct.*, **138**, 106368 (2020).
- [2] Z. Ren, Q. Sun, S.Y. Kwon, J. Han, K. Davitt, Y.K. Song, A.V. Nurmikko, H.K. Cho, W. Liu, J.A. Smart, L.J. Schowalter. *Appl. Phys. Lett.*, **91** (5), 90 (2007).
- [3] A.V. Myasoedov, D.V. Nechaev, V.V. Ratnikov, A.E. Kalmykov, L.M. Sorokin, V.N. Zhmerik. *Pis'ma ZhTF*, **46** (11), 26 (2020). (in Russian).
- [4] K. Balakrishnan, M. Iwaya, S. Kamiyama, H. Amano, I. Akasaki, T. Takagi, T. Noro. *Jpn. J. Appl. Physics, Part 1 Regul. Pap. Short Notes Rev. Pap.*, **43** (11 A), 7448 (2004).
- [5] R.R. Sumathi. *J. Solid State Sci. Technol.*, **10** (3), 035001 (2021).
- [6] T.S. Argunova, M.Y. Gutkin, E.N. Mokhov, O.P. Kazarova, J.-H. Lim, M.P. Shcheglov. *Phys. Solid State*, **57** (12), 2473 (2015).
- [7] P. Khirsh, A. Khovi, R. Nikolson, D. Peshli, M. Uelan. *Elektronnaya mikroskopiya tonkikh kristallov* (M., Mir, 1968). (in Russian).
- [8] T.S. Argunova, M.Y. Gutkin, J.H. Je, A.E. Kalmykov, O.P. Kazarova, E.N. Mokhov, K.N. Mikaelyan, A.V. Myasoedov, L.M. Sorokin, K.D. Shcherbachev. *Crystals*, **7** (6), 1 (2017).
- [9] E.N. Mokhov, I. Izmaylova, O. Kazarova, A. Wolfson, S. Nagalyuk, D. Litvin, A. Vasiliev, H. Helava, Y. Makarov. *Phys. Status Solidi Curr. Top. Solid State Phys.*, **10** (3), 445 (2013).
- [10] D. Hull and D.J. Bacon. *Introduction to Dislocations* (Butterworth-Heinemann is an imprint of Elsevier, 2011).
- [11] A.S. Grashchenko, S.A. Kukushkin, A.V. Osipov. *Izv. RAN. Mekhanika tverdogo tela*, № 2, 3 (2020). (in Russian).
- [12] J.E. Ayers. *Heteroepitaxy of Semiconductors: Theory, Growth, and Characterization* (Boca Raton, CRC Press, 2007).

*Translated by E.Potapova*